

Stable isotope paleohydrology and chemostratigraphy of the Albian Wayan Formation from the wedge-top depozone, North American Western Interior Basin

Jeffrey B. ROSS^{1*}, Greg A. LUDVIGSON², Andreas MÖLLER¹,
Luis A. GONZALEZ¹ & J. D. WALKER¹

¹Department of Geology, University of Kansas, Lawrence, Kansas 66045, USA;

²Kansas Geological Survey, University of Kansas, Lawrence, Kansas 66045, USA

Received October 11, 2016; accepted November 14, 2016; published online December 14, 2016

Abstract Understanding of the role of atmospheric moisture and heat transport in the climate system of the Cretaceous greenhouse world represents a major challenge in Earth system science. Stable isotopic paleohydrologic data from mid-Cretaceous paleosols in North America, from paleoequatorial to paleoArctic latitudes, have been used to constrain the oxygen isotope mass balance of the Albian hydrologic cycle. Over the range from 40°–50°N paleolatitude, sideritic paleosols predominate, indicating paleoenvironments with positive precipitation-evaporation (P-E) balances. Local exceptions occur on leeward side of the Sevier Orogen, where calcic paleosols in the wedge-top depozone record paleoenvironments with negative P-E balances in the orographic rain shadow. Stratigraphic sections in the Wayan Formation of Idaho (WF) were sampled from the wedge-top depozone. The units consist of stacked m-scale mudstone paleosols separated by m-scale sandstone-siltstone beds. Sections were sampled for organic carbon isotope profiles, and B-horizons from 6 well-developed paleosols were sampled for detrital zircons to determine maximum depositional ages. The first of these from the WF has produced a U-Pb concordia age of 101.0±1.1 Ma. This same WF section has produced a stratigraphic trend of upwardly decreasing $\delta^{13}\text{C}$ values ranging from –24‰ upwards to –27‰ VPDB, suggesting correlation to the late Albian C15 C-isotope segment. Pedogenic carbonates from the WF principally consist of micritic calcite, with carbon-oxygen isotope values that array along meteoric calcite lines (MCLs) with $\delta^{18}\text{O}$ values that range from –9.47‰ up to –8.39‰ VPDB. At approximately 42°N paleolatitude, these MCL values produce calculated paleoprecipitation values of –8.12‰ to –7.04‰ VSMOW, a range that is consistent with the estimates produced from other proxies at the same paleolatitudes across North America. These results indicate that despite the orographic rain shadow effect, the processes of meridional atmospheric moisture transport in this locale were similar to those in more humid mid-latitude paleoenvironments elsewhere in the continent.

Keywords Cretaceous, Paleoclimate, Wayan Formation, Pedogenic carbonates, Geochronology

Citation: Ross J B, Ludvigson G A, Möller A, González L A, Walker J D. 2017. Stable isotope paleohydrology and chemostratigraphy of the Albian Wayan Formation from the wedge-top depozone, North American Western Interior Basin. *Science China Earth Sciences*, 60: 44–57, doi: [10.1007/s11430-016-0087-5](https://doi.org/10.1007/s11430-016-0087-5)

1. Introduction

Stable isotope investigations of the Cretaceous hydrologic cycle are yielding new insights into the role of atmospheric

moisture and latent heat transport in regulating Earth surface temperatures in an ancient greenhouse world (Ufnar et al., 2002, 2004; Suarez et al., 2009, 2011; Ludvigson et al., 2013). These include stable isotope data produced from pedogenic carbonates and phosphate substrates from vertebrate fossils. Much of the published mid-latitude data comes from

*Corresponding author (email: j894r483@ku.edu)

pedogenic siderites that formed in paleo-environments with positive precipitation-evaporation (P-E) balances (Ufnar et al., 2002, 2004; Suarez et al., 2011). Within the Ferrel Cell, a zonal humid belt of the mid-latitudes, were local paleoenvironments related to orographic rain shadow effects on the leeward side of the Cretaceous Sevier orogeny (Figure 1). The Wayan Formation of eastern Idaho is a continental deposit that accumulated in this local setting.

The Wayan Formation (WF), of the Caribou Basin in Idaho, U.S.A. (Figure 2) has been described as interbedded conglomerates, sandstones, siltstones, mudstones, and limestones that were deposited on an alluvial plain (Schmitt & Moran, 1982). Strata of the WF outcrop as sub-vertically dipping beds due to faulting and folding associated with accumulation on the wedge-top depozone where deformation occurred near the depositional surface and not in a more deep burial setting (DeCelles and Giles, 1996). This alluvial plain in which the WF was deposited falls on the immediate leeward side of the Sevier Orogen. Atmospheric moisture transport by paleowesterlies would have been deflected

by the Sevier orogen and adiabatic warming of air masses descending on the leeward side of the orogen produced an orographic rain shadow as described by Elliott et al. (2007). Paleoclimate proxies at or near the same paleolatitude as the WF indicate a warm temperate climate with the development of coals and kaolinites (Boucot et al., 2013), however, within the mid-latitude orographic rain shadow, a north-south trending zone of calcrete deposits capture a record of a semiarid paleo-environment (Figure 1). The project reported here is based on ongoing research on the paleoenvironment and paleoclimate of the North American Cretaceous Western Interior Basin (WIB), following from earlier studies that deciphered the paleoenvironments, paleoecology, and paleoclimate of the Cretaceous WIB utilizing isotopic compositions of fossilized vertebrate faunas (Suarez et al., 2012, 2014), siderites (Ufnar et al., 2002), and soil carbonate nodules (Ludvigson et al., 2010). The aforementioned examples have helped further our knowledge about the paleoclimatology of the Cretaceous WIB. However, there are many anomalous locales that need to be studied to further

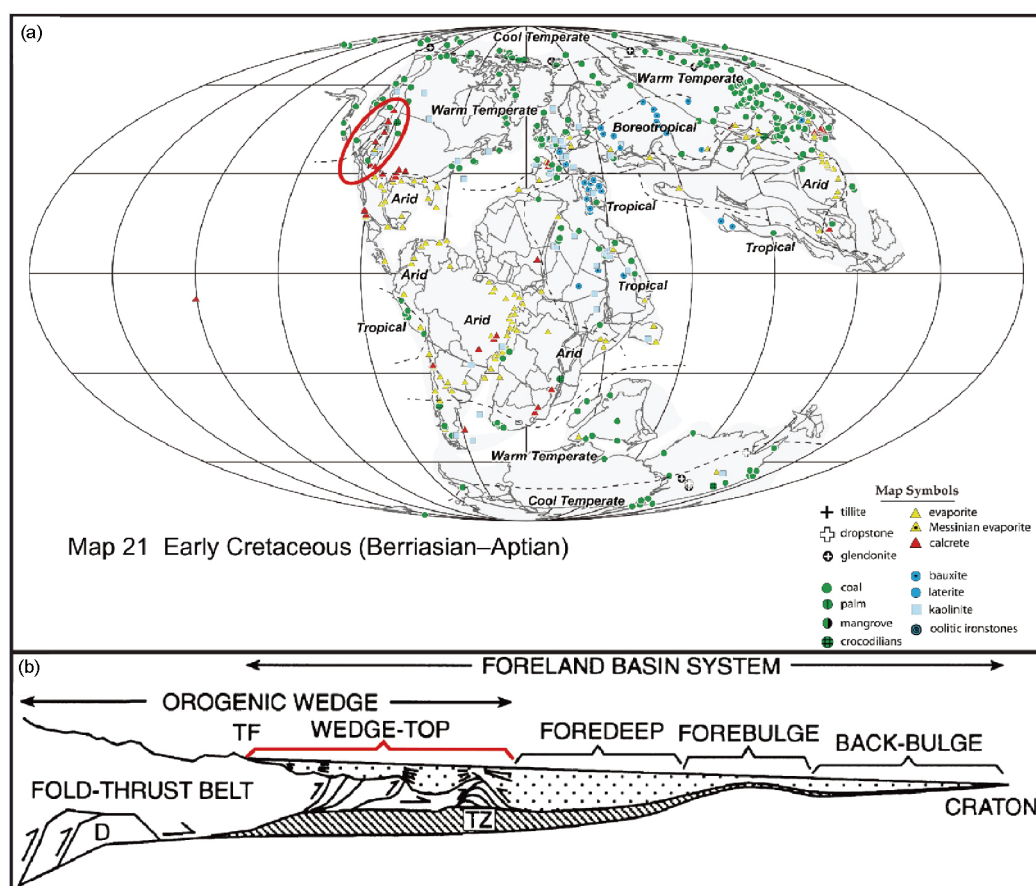


Figure 1 Tectonic and paleoclimatologic setting of the Cretaceous Wayan Formation. (a) North-south trending fairway of calcrete deposits in the rain shadow on the leeward (east) side of the Sevier orogen in western North America. This Berriasian–Aptian paleogeographic map from SEPM (Boucot et al., 2013) most clearly shows the zonal evaporation deficit of the Hadley Cell in North America to the south of 30°N paleolatitude, and the fairway of calcretes in the rain shadow of the Sevier orogen (in red oval) extending from 30° to 50°N paleolatitude. This paleogeographic map is used by permission by SEPM. Calcretes of the Wayan Formation accumulated in paleosols at 42°N paleolatitude; (b) tectonic setting of the wedge-top depozone (see red bracket) in the foreland basin system. TF, topographic front of thrust belt; D, schematic duplex; TZ, frontal triangle zone, from DeCelles and Giles (1996), used by author's permission.

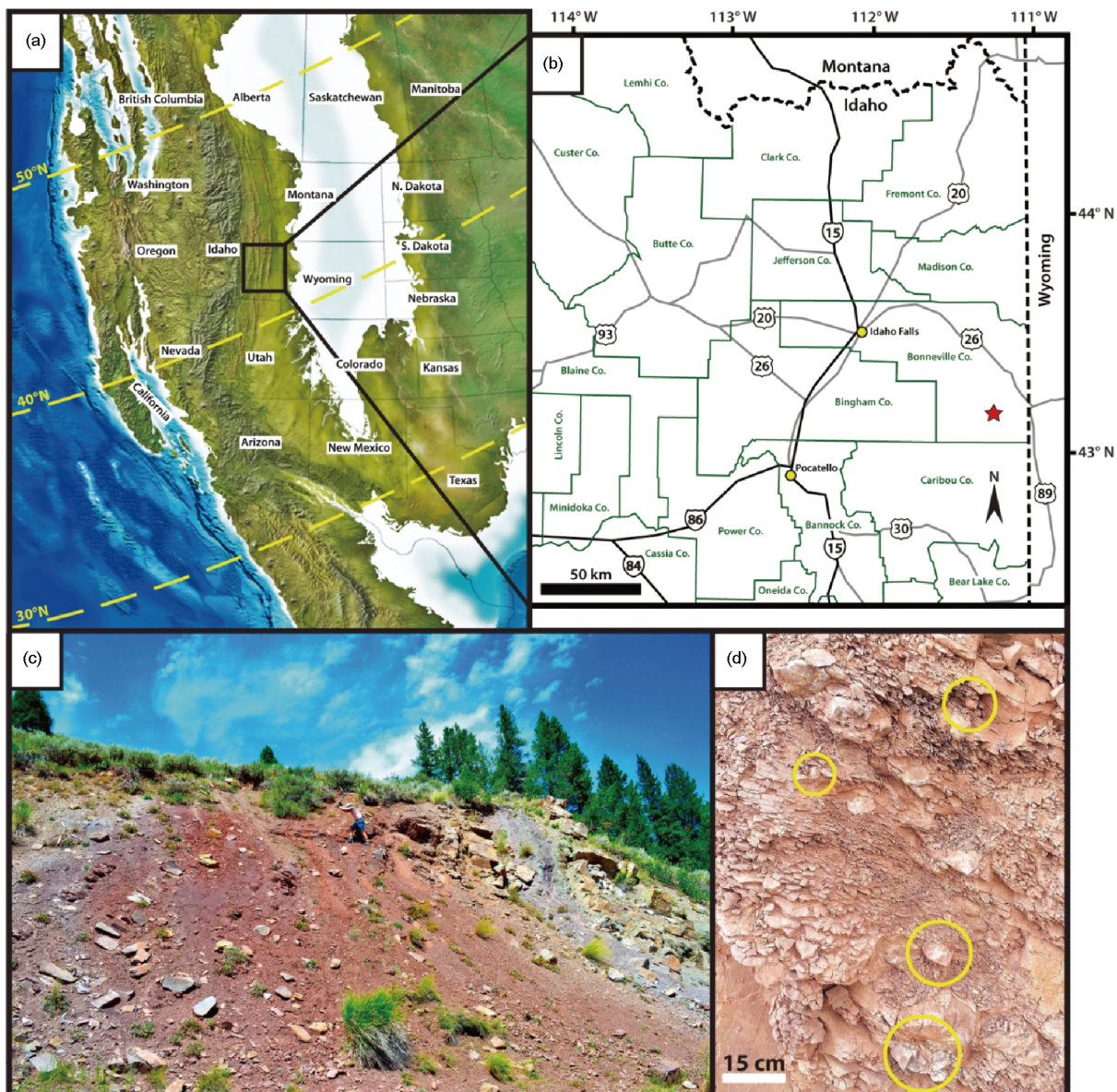


Figure 2 Location of stratigraphic section of Cretaceous Wayan Formation in the Caribou Basin, Bonneville County, Idaho. (a) Continental-scale paleogeographic map of North America during the Albian (100 Ma) from (http://cpgeosystems.com/images/WNA_100_KALb-sm.jpg) ©Ron Blakey, Colorado Plateau Geosystems, used with permission; (b) location of stratigraphic section of the Wayan Formation in the Caribou Basin (red star) in eastern Idaho; (c) field photo of the Wayan Formation on McCoy Creek Rd., in the Caribou Basin of Bonneville County Idaho, U.S.A.; (d) close up image of pedogenic texture of paleosols of the Wayan Formation with in situ carbonate nodules (in yellow circles). Field photos (c & d) have had the contrast, brightness, and color saturation altered to visually enhance their appearance. Original copies of unaltered photos may be requested of the author.

contribute to our developing knowledge of vapor transport and precipitation-evaporation (P-E) balances within the Cretaceous WIB. Pedogenic carbonate nodules that formed *in situ* within paleosols of the WF can provide isotopic data from the more semiarid paleoenvironments of the rain shadow of the Sevier orogen to contrast with previously published data.

Global chemostratigraphic profiles of marine carbonates ($\delta^{13}\text{C}_{\text{carb}}$) and organic carbon ($\delta^{13}\text{C}_{\text{org}}$) have been correlated through the Aptian-Cenomanian, identifying carbon isotope excursions (CIEs) associated with oceanic anoxic events (OAEs; Scholle and Arthur, 1980; Leckie et al., 2002). A

carbon isotope chemostratigraphic profile of the WF has been produced to compare with published profiles to expand on developing knowledge of organic carbon chemostratigraphy within the terrestrial realm. Correlating global CIEs with those identified in the chemostratigraphic profile of the WF requires integration with radiometric U-Pb dates.

Previously-published stratigraphic studies of the WF have used biostratigraphic correlations to place the WF within the Albian and Cenomanian (Krumenacker et al., 2016). Geochronological data integrated with carbon isotope chemostratigraphy of paleosols is a developing approach that

can be used to constrain time in the terrestrial realm. Previous work with volcanogenic zircons has dated the Wayan Formation to 95.5 to 101.8 Ma (Krumenacker, 2010). An important aspect of this project is U-Pb dating of zircon from paleosol horizons within a measured section to provide a maximum depositional age (MDA) of the sampled horizons.

The meteoric calcite line (MCL; *sensu* Lohmann, 1988), values obtained from carbonate nodules of the WF will be used to calculate paleoprecipitation $\delta^{18}\text{O}$ values for comparison with other published paleoprecipitation $\delta^{18}\text{O}$ values (Suarez et al., 2009). This comparison will determine whether or not paleogroundwater and paleoprecipitation $\delta^{18}\text{O}$ values from the WF are comparable to those determined from pedogenic siderites at the same paleolatitudes (42° – 43°N) elsewhere in North America. This will be the first study to determine if isotopic data from the orographic rain shadow of the Sevier orogen produces proxy data that are comparable to paleohydrologic and paleoclimatic data from more humid paleoenvironments in the Cretaceous North American mid-latitudes.

2. Methods

2.1 Wayan Formation outcrop

Sampling of the WF took place in the Caribou Basin of Bonneville County in eastern Idaho (Figure 2b). A 27 meter composite measured section was trenched perpendicular to strike which ranged from $\text{N}10^\circ\text{W}$ to $\text{N}15^\circ\text{W}$ (dip angles from 80° to 90° east) through this section along McCoy Creek Road at 43.1478°N , 111.2479°W . Trenches along the outcrop were dug to approximately 0.5 meters depth below surface to collect samples that have not been exposed to surficial weathering processes.

2.2 U-Pb geochronology of zircon

Bulk paleosol samples of 2–3 kg were collected from sample horizons in the WF that contained carbonate nodules. Samples were split to reduce bulk size to 1 kg. Due to high concentrations of calcite cement the samples were initially acidified with 1.5N HCl to aid the disaggregation process. After decarbonation, the samples were crushed and a GEMINI mineral concentration table was used to separate the majority of light minerals from the higher density minerals, including zircon. An iodine bath was used to remove remaining clays from mineral grain surfaces. Zircon was concentrated with methylene iodide heavy liquid and a Frantz isodynamic magnetic separator. A total of 310 zircon grains were hand-picked under a binocular microscope, mounted in an epoxy resin disc, and micropolished to expose grain surfaces in order to ensure analysis of the youngest stage(s) of zircon crystal growth. Some zircon grains were not analyzed due to little to no surface exposure in the epoxy resin disc.

A total of 283 zircon grains were analyzed with a Thermo Scientific Element2 ICP-MS, attached to a Photon Machines Analyte.G2 193 nm ArF excimer laser ablation system. 20 μm circular spots were ablated with 2.0 J cm^{-2} fluency and a 10 Hz repetition rate, which produced ablation pits of ca. 10 μm depth. The ablated material was carried to the ICP in He gas with a 1.11 min^{-1} flow rate. Elemental fractionation, downhole fractionation and calibration drift were corrected by bracketing measurements of unknowns with GJ1 zircon reference material (Jackson et al., 2004). Data reduction was carried out with the IOLITE software package (Paton et al., 2010, 2011) using the VizualAge data reduction scheme (Petrus and Kamber, 2012). The reproducibility of the GJ1 reference material used for calibration (Jackson et al., 2004) during the analytical session was better than 0.2% on the $^{206}\text{Pb}/^{238}\text{U}$ age (weighted average $600.4\pm 1.2\text{ Ma}$, $\text{MSWD}=0.33$, $n=58$), which was propagated into the uncertainty of the unknowns. Plesovice zircon (Sláma et al., 2008) was used as a secondary reference material to assess age accuracy and 26 concordant analyses yielded a concordia age of $340.7\pm 1.0\text{ Ma}$, with an MSWD of 0.79. This is within 1% of the thermal ionization mass spectrometry results of Sláma et al. (2008) and within error identical to the $^{206}\text{Pb}/^{238}\text{U}$ age of $340.94\pm 0.53\text{ Ma}$ determined by six other LA-ICP-MS and SIMS laboratories that yielded reliable results for a variety of reference materials in the study of Košler et al. (2013). All data obtained on 283 zircon grains are shown in Appendix table 1 (available at <http://earth.scichina.com>), but only concordant or near-concordant analyses were used for plots and calculations. The filtering for discordant analyses was done by two different calculations. For grains with $^{206}\text{Pb}/^{238}\text{U}$ dates below 900 Ma, results were excluded that had values above 1.2 for: $(^{207}\text{Pb}/^{235}\text{U}\text{ date} - ^{206}\text{Pb}/^{238}\text{U}\text{ date}) / ^{207}\text{Pb}/^{235}\text{U}$ 2SE (Standard Deviations). This takes into account that in LA-ICP-MS U-Pb analysis of young zircon, the $^{207}\text{Pb}/^{235}\text{U}$ date has a high uncertainty due to the low abundance of ^{207}Pb . For grains with $^{206}\text{Pb}/^{238}\text{U}$ dates above 900 Ma discordance % were calculated as: $(1 - (^{207}\text{Pb}/^{206}\text{Pb}\text{ date} / ^{206}\text{Pb}/^{238}\text{U}\text{ date})) \times 100$ and data more than 5% discordant were excluded from plots and further discussion. Of the 283 results 209 analyses passed these two discordance filters.

2.3 Pedogenic carbonate nodules

Pedogenic carbonate nodules were collected from 7 well developed paleosol B-horizons of the WF. Matching micropolished thin and thick sections were cut from epoxy resin-impregnated billets for petrographic analysis. Cathodoluminescence imaging (CL) was used to identify variably luminescent and non-luminescent calcite components on thick sections. Photomicrographs were produced in CL and mapped onto reflected light (RL) images to guide microsampling of various calcite components for $\delta^{13}\text{C}$ and $\delta^{18}\text{O}$ analyses (Figure 3a–c).

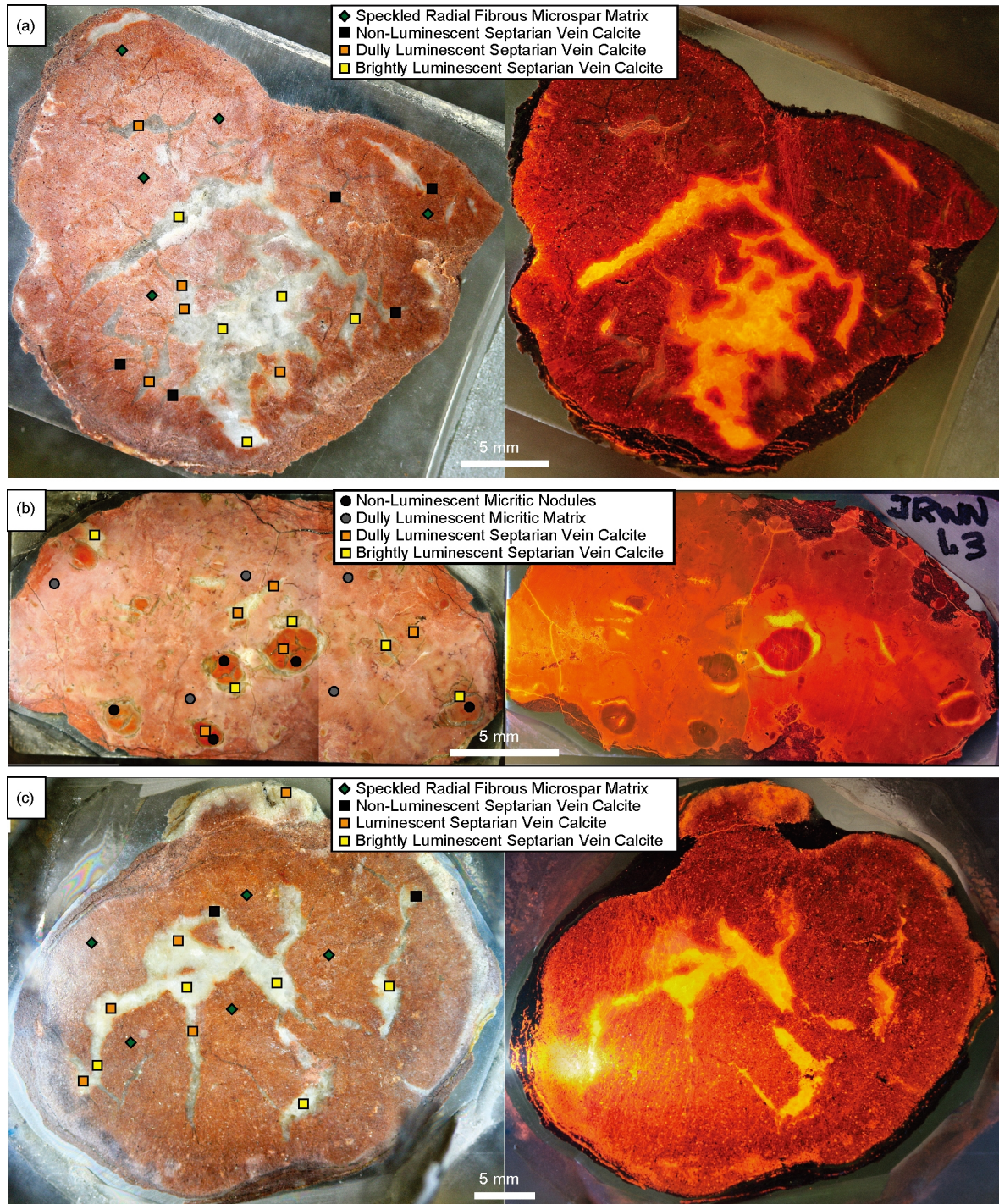


Figure 3 Matching reflected light (left) and cathodoluminescence (right) images of micropolished thick sections slabbed from pedogenic calcite nodules sampled from the Wayan Formation at Caribou Basin. Individual calcite components and the locations of microsamples extracted from the thick sections are labelled on the reflected light images, and include CL non-luminescent micritic nodule matrix, CL dully luminescent nodule matrix, CL speckled radial fibrous microspar nodule matrix, CL non-luminescent septarian vein calcite, CL dully luminescent septarian vein calcite, and CL brightly luminescent septarian vein calcite. (a) Pedogenic calcite nodule from Wayan 1.2 as shown in Figure 5; (b) pedogenic calcite nodule from Wayan 1.3 as shown in Figure 5; (c) pedogenic calcite nodule from Wayan 1.5 as shown in Figure 5.

Results of $\delta^{13}\text{C}$ and $\delta^{18}\text{O}$ are reported in delta notation (δ) per mil (‰) in deviation on the Vienna Pee Dee Belemnite (VPDB) scale with analytical precision better than 0.18‰.

Cathodoluminescence imaging was carried out at the

Kansas Geological Survey Digital Cathodoluminescence Imaging Laboratory using a Reliotron III cold cathode chamber mounted on a Relion Industries table top stand. Macroimages were captured with a Canon EOS Xti 10.1

Mpx DSLR using a Canon EFS 60 mm f/2.8 macro USM lens mounted on a boom stand suspended over the CL chamber. CL images were captured in operating conditions that consisted of an electron beam voltage of 10 kV, a beam current of 0.5 mA, and in a chamber with rarified Helium atmosphere at 50 milli Torr.

Pedogenic carbonate components were micro-sampled at The University of Kansas Keck-NSF Paleoenvironmental and Environmental Laboratory. Each carbonate component identified was sampled from 2 to 5 separate locations on each nodule. A minimum of 100 μg of sample was collected from each sample location (Figure 3) and was shipped to the University of Michigan Stable Isotope Laboratory for analyses on a Finnigan MAT 251 coupled to a Finnigan Kiel automated preparation device. Crossplots of $\delta^{13}\text{C}$ and $\delta^{18}\text{O}$ values were made and used to interpret diagenetic history for sampled nodules (Figure 4).

2.4 Organic carbon isotopes

A 27 meter section of the Wayan Formation was sampled at 0.5 meter intervals for organic carbon isotope analyses. Samples were ground in a ceramic mortar and pestle and dried over a 24 hour period before being placed into centrifuge tubes. Tubes were weighed before and after adding samples to allow for a total organic carbon (TOC) percent to be calculated after analyses. Samples were then acidified with 0.5 N HCl to remove carbonate and leached to a neutral pH. Acidified samples were combusted in Costech Elemental Analyzer coupled to continuous-flow ThermoFinnigan MAT 253 stable isotope ratio mass spectrometer at the Keck Paleoenvironmental & Environmental Stable Isotope Laboratory at The University of Kansas to produce organic $\delta^{13}\text{C}$ analyses. Standards used to calibrate the $\delta^{13}\text{C}$ the analyses were USGS-24 (graphite), DORM (dogfish muscle), IAEA-600 (caffeine), ANU (sucrose), MT soil, and Peach Leaf. The organic carbon $\delta^{13}\text{C}$ values are plotted with stratigraphic profiles to assess the chemostratigraphic structure of studied units (Figure 5). Results of analyses are reported in delta notation (δ) per mil (‰) in deviation on the Vienna Pee Dee Belemnite (VPDB) scale with analytical precision better than 0.1‰.

3. Results

3.1 Petrography and stable isotope data for pedogenic carbonates

Two hundred eighty three U-Pb analyses were performed by LA-ICP-MS on detrital zircon from the WF obtained from sample location WN1.5 at 11.6 meters above the base of the section (Figure 5). A total of 209 of the analyzed grains passed the concordance criteria outlined in the methods chap-

ter above, and 58 of these are younger than 200 Ma (Figure 6a). Fifty five of these fall in a narrow range of latest Early Cretaceous (Albian) age with $^{206}\text{Pb}/^{238}\text{U}$ ages from 99.7 to 113.2 Ma (Figure 6a), whereas only one Aptian, one Late Jurassic and one Early Jurassic grain were found. A U-Pb Concordia age of 101.0 ± 1.1 Ma was calculated from the youngest 3 concordant zircon analyses overlapping within 2σ (Figure 6b), which is interpreted as the best estimate for the maximum depositional age (MDA) of the sampled stratum, which is based on the most conservative estimate of MDA (after the strategy proposed by Dickinson and Gehrels, 2009). The distribution of results within the Early Cretaceous population is shown in a kernel density plot (kdp) produced with the DensityPlotter software (Vermeesch, 2012), shows a major age distribution maximum at ca. 105 Ma, with a slightly skewed distribution and a local maximum of results at ca. 110 Ma (Figure 6c).

Among the pre-Cretaceous zircon grains, only one late Triassic (Rhaetian) zircon, and no concordant zircons with ages between 205 and 300 Ma were found. The full distribution of concordant detrital zircons with ages between 130 Ma and 3.0 Ga is shown in a kdp in Figure 6d.

The oldest concordant analysis (3671 ± 87 Ma) is not shown in Figure 6d to conserve space in the figure. Notable maxima in the age distribution are found in the Late Devonian at ca. 380 Ma, early Silurian at ca. 440 Ma, and early Ediacaran at 600 to 650 Ma. Lower abundances of grains were found to have a broad distribution of ages between ca. 800 and 2000 Ma. The most prominent of these small maxima is at ca. 1.6–1.7 Ga. Isolated single zircons with ages at 2.2, 2.6, and 2.7 Ga, and 2 analyses at 2.8 Ga were obtained.

Pedogenic carbonates from sample WN1.2 consist of nodule matrix components that are characterized by radial fibrous microspar with micron-scale speckled CL luminescence, and with long crystal dimensions from 100 to 800 μm (Figure 3a). Septarian veins contained within nodules from WN1.2 are filled by zoned calcite spars with distinctive CL characteristics. The first of these, Zone 1 consists of non-luminescent septarian vein calcites with equant crystal dimensions of about 100–200 μm that are present on the edges of septarian veins and matrix components, and completely fill smaller septarian veins (Figure 3a). The following Zone 2 consists of CL dully luminescent equant calcite crystals with dimensions ranging from 100 to 500 μm that are present in larger septarian veins between Zone 1 and zone 3 septarian veins (Figure 3a). The later Zone 3 consists of CL brightly luminescent equant calcite crystals with dimensions ranging from 500 to 2000 μm and occur as the final phase of septarian vein calcite crystal growth (Figure 3a).

Pedogenic carbonate nodules from sample WN1.3 consist of smaller nodules with a CL non-luminescent micritic matrix calcite, with crystal dimensions of less than 10 μm ; these

smaller nodules are encompassed within larger nodules with CL dully-luminescent micritic matrix, with crystal dimensions less than 20 μm (Figure 3b). Nodules from WN1.3 also contain zoned septarian veins that are filled by successive

zones of calcite spars with distinctive CL characteristics. The earliest Zone 1 consists of dully luminescent equant calcite with crystal dimensions ranging from 50 to 250 μm —these occur within the septarian veins of smaller micritic nod-

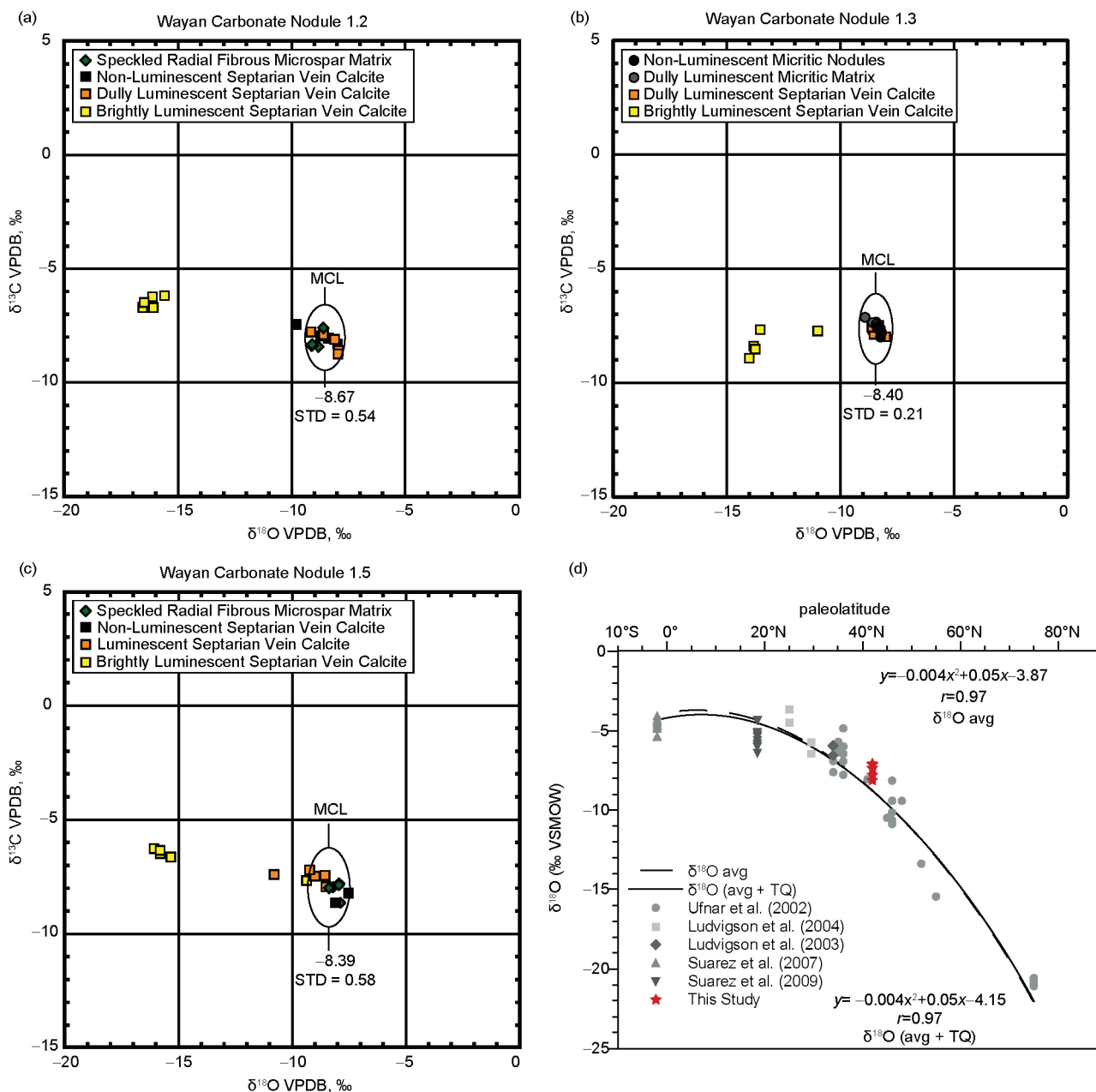


Figure 4 Carbon and oxygen isotope plots of calcite components from pedogenic calcite nodules in the Wayan Formation at Caribou Basin, Idaho. Nodule matrix calcites have relatively invariant $\delta^{18}\text{O}$ values conforming to the pattern of meteoric calcite lines (MCLs), with arithmetic means of -8.67‰ , -8.40‰ , and -8.39‰ VPDB, with standard deviations ranging from 0.2‰ up to 0.58‰. Early-formed non-luminescent and dully luminescent vein calcites have carbon and oxygen isotope values that are closely similar to those of the MCL values of the matrix calcites, but the later-formed brightly luminescent septarian vein calcites have much lower $\delta^{18}\text{O}$ values ranging from -17‰ to -11‰ VPDB. (a) Carbon and oxygen isotope plot of calcite components from pedogenic calcite nodule Wayan 1.2 as shown in Figure 3; (b) carbon and oxygen isotope plot of calcite components from pedogenic calcite nodule Wayan 1.3 as shown in Figure 3; (c) carbon and oxygen isotope plot of calcite components from pedogenic calcite nodule Wayan 1.5 as shown in Figure 3. (d) Cretaceous (Albian) paleolatitudinal transect of the Americas showing calculated groundwater/paleoprecipitation $\delta^{18}\text{O}$ values from Suarez et al. (2009; used by author's permission) and the groundwater/paleoprecipitation $\delta^{18}\text{O}$ values calculated from MCL values derived from pedogenic carbonates in the Wayan Formation (red stars, this study). The calculated paleoprecipitation values from Wayan Formation at 42°N paleolatitude appear to have a close fit to the polynomial regression of Suarez et al. (2009).

ules contained within the larger nodules, and also within septarian veins of the encompassing larger nodules (Figure 3b). The later Zone 2 consists of CL brightly-luminescent equant

crystals with dimensions ranging from 100 and 800 μm that occur in the largest septarian veins within the larger micritic nodules (Figure 3b).

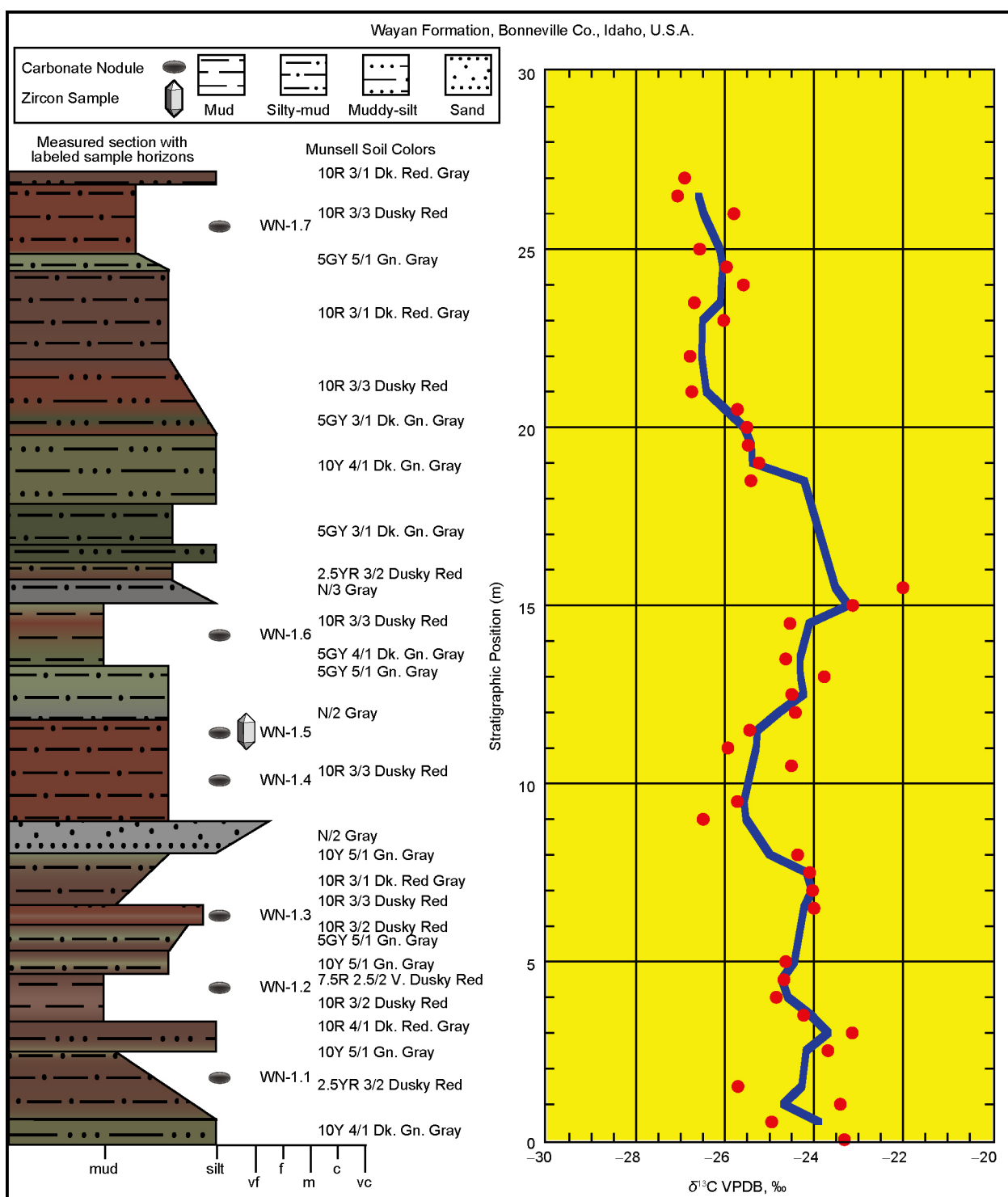


Figure 5 Graphic log and organic carbon isotope stratigraphy of exposed 27 meter section of the Wayan Formation at Caribou Basin in Bonneville County, Idaho. To the left, sediment particle sizes ranging from mudstones-siltstones up to fine-grained sandstones are shown in the profile of the graphic log. Munsell soil colors are coded to the right of the graphic log, and are mimicked in the soil colors of the graphic log. Horizontal ellipses and a zircon symbol to the right of the graphic log show the positions of sampled pedogenic carbonates and horizon sampled for U-Pb dating of zircon. To the right, the organic carbon isotope profile shows individual analyses in red dots, along with the three-point moving average in blue line.

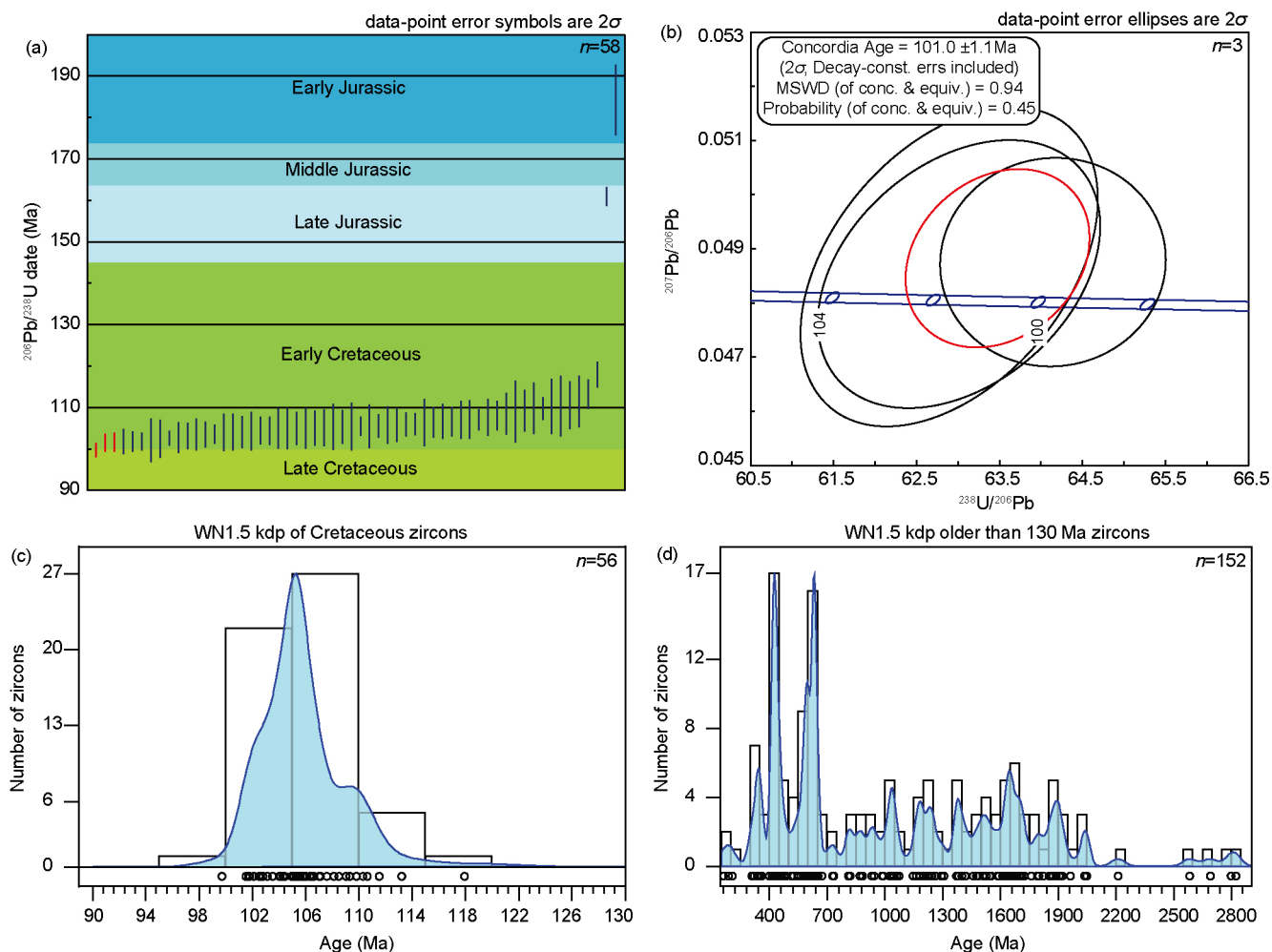


Figure 6 Diagrams for the results from U-Pb dating of zircon from sample WN1.5. (a) $^{206}\text{Pb}/^{238}\text{U}$ dates with 2σ error bars for the 58 youngest analyses, between 90 and 200 Ma, shown on a color-coded geological time scale (Walker et al., 2013). The plot shows a near-continuous range of overlapping dates between ca. 100 and 114 Ma, only 3 grains with dates between 115 and 190 Ma were identified. The three youngest overlapping results (in red) were used to calculate the maximum depositional age (MDA), following the reasoning of Dickinson and Gehrels (2009). (b) Tera-Wasserburg concordia diagram (Tera and Wasserburg, 1972) for the three youngest results overlapping within 2σ . The resulting concordia age of 101.0 ± 1.1 Ma is interpreted as the best estimate for the MDA of this sample, placing it near the end of the Albian Age, and thereby the end of the Early Cretaceous Epoch. (c) and (d) Kernel density plots (kdp) for 208 from a total of 209 concordant analyzed grains: (c) a kdp for the 58 concordant analyses between ca. 100 and 130 Ma. Plotted are the $^{206}\text{Pb}/^{238}\text{U}$ dates; (d) kdp for the analyses between 150 and 3000 Ma. Plotted are $^{206}\text{Pb}/^{238}\text{U}$ dates up to 900 Ma, $^{207}\text{Pb}/^{206}\text{Pb}$ dates are plotted for older grains. Note the paucity of Jurassic, Triassic and Permian grains.

Pedogenic carbonates from sample WN1.5 consists of nodule matrix components that display a radial fibrous microspar characterized by a micron-scale speckled CL luminescence, with long crystal dimensions from 100 to 800 μm (Figure 3c). Septarian veins contained within nodules from WN1.5 are filled by zoned calcite spars with distinctive CL characteristics. The earliest Zone 1 consists of non-luminescent septarian vein calcites with equant crystal dimensions of about 100–200 μm , and are present along the edges of matrix components along vein walls (Figure 3c). The later Zone 2 consists of CL luminescent equant calcite crystals with dimensions ranging from 100 to 500 μm that are present in larger septarian veins between Zones 1 and 3 (Figure 3c). Zone 3 consists of CL brightly luminescent equant calcite crystals with dimensions ranging from 500 to 2000 μm and occurs

in the centers of larger septarian veins as the final phase of calcite crystal growth (Figure 3c).

Zones of carbonate diagenesis outlined here for each carbonate nodule horizon within the WF may be similar to nodules from other stratigraphic horizons, however, each stratigraphic horizon containing carbonate nodules within the WF exhibit a paragenesis that is independent of nodules from other stratigraphic horizons. Carbonate nodules from the Wayan Formation have $\delta^{18}\text{O}$ values that range from $-9.47\text{‰} \pm 0.64\text{‰}$ up to $-8.39\text{‰} \pm 0.21\text{‰}$ VPDB; and $\delta^{13}\text{C}$ values that range from $-8.74\text{‰} \pm 0.37\text{‰}$ up to $-7.13\text{‰} \pm 0.24\text{‰}$ VPDB, with three examples of carbon-oxygen isotope plots shown in Figure 4. Brightly-luminescent septarian vein calcites (Zone 3) have notably lower $\delta^{18}\text{O}$ values ranging from -16.56‰ to -10.93‰ VPDB, while the $\delta^{13}\text{C}$ values of Zone

3 calcites are similar to those of the enclosing finer-grained matrix calcites (Figure 4a–c). Matrix calcite components that produce relatively invariant oxygen isotope values are arrayed along meteoric calcite lines (MCLs; *sensu* Lohmann, 1988), a pattern that can develop in pedogenic calcites in modern surface soils (Mintz et al., 2011).

3.2 Organic carbon isotope chemostratigraphy

The range of $\delta^{13}\text{C}$ values obtained from organic carbon analyses is -27.07‰ to -22.00‰ VPDB with total organic carbon (TOC) ranging from 0.03% to 0.34%. A $\delta^{13}\text{C}_{\text{org}}$ chemostratigraphic profile of the WF (Figure 5) displays a stratigraphic upward trend from higher values at the base (about -23‰ VPDB) to lower values at the top of the section (about -27‰ VPDB). Several minor carbon isotope fluctuations can be seen within the $\delta^{13}\text{C}_{\text{org}}$ profile, specifically at the 9 meter interval where there is a negative shift to -26.49‰ VPDB followed by a maximum positive shift at the 15.5 meter interval to -22.0‰ VPDB before returning to a negative trend to the end of the profile. However, the chronostratigraphic significance of these features is uncertain without additional geochronologic data from other parts of the sampled section.

4. Discussion

4.1 Stable isotope paleohydrology of pedogenic carbonates

The paragenetic sequence of carbonate diagenesis in the nodules was initiated by precipitation of carbonate matrix components. Early non-luminescent septarian vein calcites precipitated within a shallow phreatic groundwater system on the basis of equant crystal morphologies; later brightly luminescent septarian vein calcites precipitated in deeper phreatic groundwater setting where higher concentrations of Mn^{2+} in anoxic pore fluids were incorporated within septarian vein calcites.

Primary calcite components from pedogenic nodules in the Wayan Formation that capture early diagenetic paleohydrologic information are the CL non-luminescent to CL dully luminescent micritic matrix, and radial fibrous microspars with CL speckled luminescence (Figure 3a–c). These components yield carbon and oxygen isotope values that array along MCL trends, and precipitated from shallow groundwaters sourced from infiltrating paleoprecipitation in the ancient vadose zones of mid-Cretaceous paleosols. Zone 1 non-luminescent spars filling septarian veins have carbon and oxygen isotope values that are similar to matrix carbonates. Post-burial diagenetic components are represented by septarian vein calcites, Zone 2 CL luminescent and Zone 3 CL brightly luminescent spars (Figure 3a–c). These later diagenetic components formed in anoxic groundwaters that incorporated reduced manganese into the calcite

crystal lattice. Paleohydrologic interpretations for individual stratigraphic horizons are developed through the analysis of specific diagenetic trends identified in $\delta^{13}\text{C}$ and $\delta^{18}\text{O}$ cross plots, and are unique to each studied rock sample (Figure 4a–c). Diagenetic trends include meteoric calcite lines (MCLs) that preserve records of the $\delta^{18}\text{O}$ compositions of infiltrating paleoprecipitation (Lohmann, 1988; Ludvigson et al., 2010). Later diagenetic trends include the records of burial diagenesis captured by Zone 3 CL brightly luminescent septarian vein calcite spars, showing a trend toward isotopically lower $\delta^{18}\text{O}$ values. Zone 3 calcite spars have similar $\delta^{13}\text{C}$ values as the matrix calcites, suggesting formation in a rock-dominated diagenetic system (Figure 4a–c). This O-isotopic value could be indicative of infiltration of groundwaters sourced by alpine snowmelt, or alternatively, could be indicative of precipitation at higher burial temperatures, as posited by Ludvigson et al. (2010).

The paleolatitude of 42°N for the Wayan Formation was estimated based on paleogeographic reconstructions of Aptian-Albian North America by Ufnar et al. (2004). The local mean annual paleotemperature (MAT) was calculated from the second-order polynomial regression generated by Ufnar et al. (2002) based on a Cretaceous latitudinal temperature gradient reported by Spicer and Corfield (1992) and fossil leaf physiognomy data of Wolfe and Upchurch (1987). This same approach was used by Suarez et al. (2009): $t = 30.25 - 0.2025l - 0.0006l^2$, where t is temperature in degrees Celsius, and l is latitude, produced a MAT of 21.74°C . Using this paleotemperature, the $\delta^{18}\text{O}$ VPDB MCL values from the WF can be used to calculate $\delta^{18}\text{O}$ VSMOW values of infiltrating paleoprecipitation. The ^{18}O fractionation factor (α) of calcite-water used, with the estimated paleotemperature (21.74°C), was taken from the relationship reported by Friedman and O'neil (1977) to determine the $\delta^{18}\text{O}$ values of meteoric fluids from the Wayan Formation. MCL values from carbonate matrix components from nodules of the WF yield estimated meteoric water values that range from -8.12‰ to -7.04‰ VSMOW (Figure 4d). These estimated groundwater $\delta^{18}\text{O}$ values are consistent with those estimated by Ufnar et al. (2002) from pedogenic siderites, from pedogenic calcites (Ludvigson et al., 2004), and $\delta^{18}\text{O}$ isotopic data from vertebrate fossil phosphate substrates (Suarez et al., 2012, 2014).

4.2 Organic carbon isotope chemostratigraphy

With the maximum depositional age (MDA) determined at 101.0 ± 1.1 Ma near the end of the Albian Stage, it is possible to accurately correlate CIEs of the WF with established global Aptian-Albian chemostratigraphic profiles (Figure 7). The magnitude of $\delta^{13}\text{C}$ shifts in C15 C-isotope segment in the marine sections (less than 1‰) is much less than comparable shifts in the terrestrial section in the Wayan Formation (greater than 2‰). This observation is compatible with those

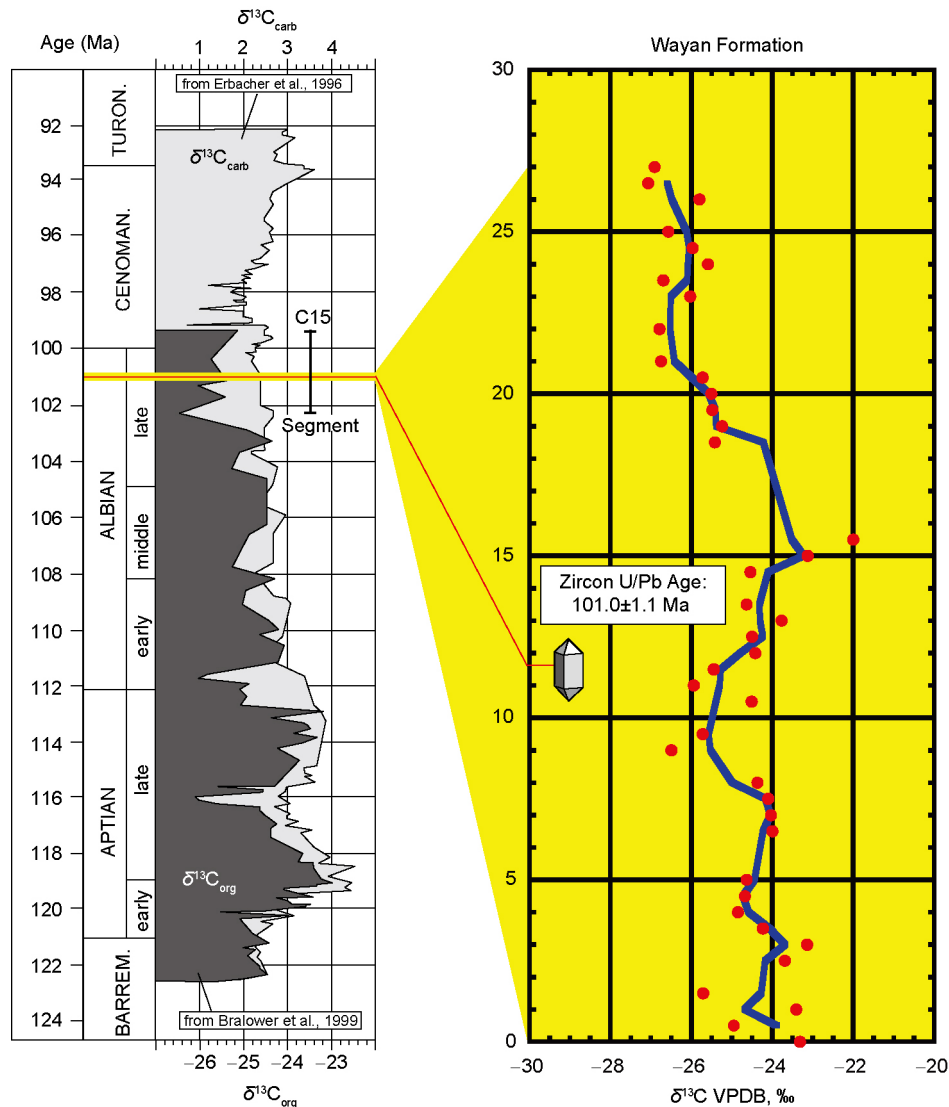


Figure 7 Aptian-Albian $\delta^{13}\text{C}$ chemostratigraphic profiles (left) from Leckie et al. (2002, used with author's permission) compared with $\delta^{13}\text{C}$ chemostratigraphic profile from the Wayan Formation (right). Note: Albian-Cenomanian boundary of Leckie et al. (2002) has been adjusted from 99 to 100 Ma to reflect the Geological Society of America time scale of Walker et al. (2013). U-Pb age of 101.0 ± 1.1 Ma (red line) obtained from zircon sample at 11.6 m interval in the Wayan Formation section correlates to the C15 C-isotope segment reported by Bralower et al. (1999). A distinctive positive $\delta^{13}\text{C}$ shift of about 2.5‰ occurs from 14.5 to 15.5 m levels, followed by a declining trend through the rest of the measured section to a final value -27% VPDB.

of Bains et al. (2003) noting that the magnitudes of terrestrial carbon isotope excursions associated with the PETM are greater than those of coeval marine carbon isotope excursions, considered to be a buffering effect of the larger carbon reservoir in the ocean basins. Samples taken from the Wayan Formation for $\delta^{13}\text{C}_{\text{org}}$ analyses did not contain evidence of macroscopic plant matter or black carbons resulting from combustion that would enrich $\delta^{13}\text{C}$ values (Gröcke et al., 2006) and are interpreted based on the analytical results.

The base of the WF $\delta^{13}\text{C}$ chemostratigraphic profile, beginning at the 0 m height, shows a general decreasing isotope trend from -23.32% to -26.49% VPDB over a 9 meter interval (Figure 7). Above this trend of decreasing values,

a positive isotope trend occurs up to the 14.5 meter interval with an abrupt increase over the next two samples positions to the 15.5 meter sample interval, where the most positive $\delta^{13}\text{C}$ value occurs of -22% VPDB (Figure 7). Following this high value, there is an upward trend of decreasing $\delta^{13}\text{C}$ values through the remainder of the section to ending values of about -27% VPDB (Figure 7). The MDA of 101.0 ± 1.1 Ma established from detrital zircons obtained from the 11.6 m interval of the $\delta^{13}\text{C}$ profile of the WF permits correlation with global Aptian-Albian $\delta^{13}\text{C}$ profiles of Leckie et al. (2002) in the late Albian, and intersect with $\delta^{13}\text{C}_{\text{org}}$ C15 C-isotope segment identified by Bralower et al. (1999). The C15 C-isotope segment of Bralower et al. (1999) has two minor negative C isotope shifts occurring within an overall positive C iso-

tope trend (Figure 7). The MDA obtained from detrital zircon U-Pb age of 101.0 Ma places the WF $\delta^{13}\text{C}$ profile between the two minor negative shifts of the Bralower et al. (1999) C15 C-isotope segment (Figure 7).

The $\delta^{13}\text{C}$ decrease in the WF C-isotope profile occurring up to the 9 meter interval might be correlated with the first C15 negative shift, with the most positive C-isotope value recorded at the 15.5 meter interval of the WF correlating with the following positive shift from Bralower et al. (1999). The upper 11.5 meters of the WF $\delta^{13}\text{C}$ profile shows an overall declining $\delta^{13}\text{C}$ trend, and may correlate with the second minor negative shift within the C15 isotope segment of Bralower et al. (1999). With 5 other zircon samples currently being processed, the full $\delta^{13}\text{C}$ profile of the WF can be more confidently correlated with global Aptian-Albian $\delta^{13}\text{C}$ chemostratigraphic profiles to further constrain time in the WF.

4.3 U-Pb geochronology of WF zircons

The abundant Albian zircon population (26% of all concordant analyses) is interpreted to reflect the highly active magmatic arc in very proximal westerly distance from the sample location (e.g. Figure 2a). The paucity of earlier Mesozoic and Permian zircons may reflect the general east- and northward transport direction at the sample location that prevented capture of any zircons from a source east of the North American Cretaceous Western Interior Seaway during this time period. Carboniferous and older zircons could have been transported far west from the East during earlier times when different transport directions dominated, and then redistributed later, as proposed e.g. by Blum and Pecha (2014) for the presence of Appalachian-age zircon throughout the Midwestern US and Central Canada. The pattern of Proterozoic zircon in the WN1.5 sample from Idaho generally matches very well with detrital zircon data from Albian strata from the Western Canada Sedimentary Basin in Northern Alberta (Blum and Pecha, 2014), with moderate amounts of Grenvillian, Mid-Continent and Yavapai-Mazatzal input. The Early Proterozoic to Eoarchean oldest obtained ages may be derived from relatively proximal underlying basement sources, the Wyoming province in the southeast or the Medicine Hat Block directly to the west and their adjacent Early Proterozoic orogenic belt neighbors (see Whitmeyer and Karlstrom, 2007), although Eoarchean material is generally extremely rare. During the mid-Cretaceous through the Paleocene there was a continual increase of magmatic activity along the western margin of North America as an Andean magmatic arc developed (Armstrong and Ward, 1993). With a zircon analysis of 283 grains, yielding an MDA of 101.0 \pm 1.1 Ma in conjunction with increasing magmatism through the Cretaceous, it is highly unlikely that any bias in sampling may have occurred, and that any zircon grains younger than the established MDA

are present in the Wayan Formation at this stratigraphic position (Vermeesch, 2004).

5. Conclusions

Pedogenic carbonate nodules of the Wayan Formation produce carbon and oxygen isotope data that array along meteoric calcite lines (MCLs), with $\delta^{18}\text{O}$ values ranging from $-9.47\text{‰}\pm 0.35\text{‰}$ to $-8.39\text{‰}\pm 0.58\text{‰}$ VPDB. These MCL values produce calculated meteoric water values ranging from -8.12‰ to -7.04‰ VSMOW. Estimated paleoprecipitation/paleogroundwater $\delta^{18}\text{O}$ values from the Wayan Formation are similar to those estimated from other published Albian paleoprecipitation proxies at about 42°N paleolatitude. These results suggest that meridional atmospheric moisture transport in the rain shadow on the leeward side of the Cretaceous Sevier Mountain was similar to that elsewhere in the North American Western Interior Basin.

Mudstone paleosols of the Wayan Formation produce an organic carbon isotope chemostratigraphic profile which exhibits an overall decreasing trend from bottom to top.

A U-Pb concordia age of 101.0 \pm 1.1 Ma was calculated from a bulk paleosol sample at the 11.6 meter horizon from the Wayan Formation. The 101.0 Ma age was produced from the youngest 3 concordant detrital zircons overlapping within 2σ . Following the logic of Dickinson and Gehrels (2009), 101.0 \pm 1.1 Ma is proposed as the maximum depositional age for this sample horizon and facilitates correlation of the $\delta^{13}\text{C}$ profile from the Wayan Formation to the global Cretaceous C-isotope stratigraphy.

Applying the MDA of 101.0 \pm 1.1 Ma to the $\delta^{13}\text{C}$ profile of the Wayan Formation (WF), comparison to the global Cretaceous (Aptian-Albian) C-isotope stratigraphy indicates that the WF $\delta^{13}\text{C}$ profile correlates to the C15 C-isotope segment identified by Bralower et al. (1999). Within the $\delta^{13}\text{C}$ profile of the WF there are more short-term trends of decreasing and increasing $\delta^{13}\text{C}$ values that might correlate to minor C-isotope shifts within the C15 C-isotope segment of Bralower et al. (1999). More geochronologic data are needed to further constrain the chronostratigraphy of these C-isotope trends.

Acknowledgements I would like to thank my field assistant, Stephan Oborny, for his help trenching and collecting samples, Luke Miller for his assistance processing samples. I would also like to thank Ted Dyman for walking me through a section of the Blackleaf Formation, and L. J. Krumenaker and Dave Varricchio of Montana State University for assistance in locating suitable Wayan Formation outcrops. And thanks to: Adrienne Duarte, Tony Layzell, Josh Feldman, Ty Tenpenny, and Maggie Graham for the training they provided to help me process samples. I would like to personally thank my advisor, Greg Ludvigson for the support he provided when work was not proceeding as planned. Many thanks to my committee members, Dr. González, Dr. Möller, and Dr. Walker for the help they provided in data interpretations. We thank Stuart Robinson, Marina Suarez, and an anonymous peer reviewer for constructive suggestions that improved our presentation. This paper is

a contribution of IGCP Project 609 "Climate-environmental deteriorations during greenhouse phases: Causes and consequences of short-term Cretaceous sea-level changes".

References

- Armstrong R L, Ward P L. 1993. Late Triassic to earliest Eocene magmatism in the North American Cordillera: implications for the western interior basin. In: Caldwell W G E, Kauffman E G, eds. *Evolution of the Western Interior Basin*. Geological Association of Canada Special Paper, 39: 49–72
- Bains S, Norris R D, Corfield R M, Bowen G J, Gingerich P D, Koch P L. 2003. Marine-terrestrial linkages at the Paleocene-Eocene boundary. *Special Papers-Geological Society of America*, 369: 1–10
- Blakey R. 2014. Library of Paleogeography. Retrieved April 4, 2016, from Colorado Plateau Geosystems, Inc.: http://cpgeosystems.com/images/WNA_100_KAlb-sm.jpg
- Blum M, Pecha M. 2014. Mid-Cretaceous to Paleocene North American drainage reorganization from detrital zircons. *Geology*, 42: 607–610
- Boucot A J, Xu C, Scotese C R. 2013. Phanerozoic paleoclimate: an atlas of lithologic indicators of climate. *Concepts in Sedimentology and Paleontology 11: SEPM (Society for Sedimentary Geology)*: 216–217. Tulsa, OK, U.S.A
- Bralower T, CoBabe E, Clement B, Sliter W V, Osburn C L, Longoria, J. 1999. The record of global change in mid-Cretaceous (Barremian-Albian) sections from the Sierra Madre, northeastern Mexico. *J Foram Res*, 29: 418–437
- DeCelles P G, Giles K A. 1996. Foreland basin systems. *Basin Res*, 8: 105–123
- Dickinson W R, Gehrels G E. 2009. Use of U–Pb ages of detrital zircons to infer maximum depositional ages of strata: A test against a Colorado Plateau Mesozoic database. *Earth Planet Sci Lett*, 288: 115–125
- Elliott W S, Suttner L J, Pratt L M. 2007. Tectonically induced climate and its control on the distribution of depositional systems in a continental foreland basin, Cloverly and Lakota Formations (Lower Cretaceous) of Wyoming, U.S.A.. *Sedimentary Geol*, 202: 730–753
- Erbacher J, Thurow J, Littke R. 1996. Evolution patterns of radiolaria and organic matter variations: A new approach to identify sea-level changes in mid-Cretaceous pelagic environments. *Geology*, 24: 499–502
- Friedman I, O'neil J R. 1977. Data of geochemistry: Compilation of stable isotope fractionation factors of geochemical interest. Geological Survey Professional Paper 440-KK. US Government Printing Office
- Gröcke DR, Ludvigson G A, Witzke B L, Robinson S A, Joeckel R M, Ufnar D F, Ravn R L. 2006. Recognizing the Albian-Cenomanian (OAE1d) sequence boundary using plant carbon isotopes: Dakota Formation, Western Interior Basin, USA. *Geology*, 34: 193
- Jackson S E, Pearson N J, Griffin W L, Belousova E A. 2004. The application of laser ablation-inductively coupled plasma-mass spectrometry to *in situ* U–Pb zircon geochronology. *Chem Geol*, 211: 47–69
- Košler J, Sláma J, Belousova E, Corfu F, Gehrels G E, Gerdes A, Horstwood M S A, Sircombe K N, Sylvester P J, Tiepolo M, Whitehouse M J, Woodhead J D. 2013. U–Pb Detrital Zircon Analysis—Results of an Inter-laboratory Comparison. *Geostand Geoanal Res*, 37: 243–259
- Krumenacker L J. 2010. Chronostratigraphy and paleontology of the mid-Cretaceous Wayan Formation of eastern Idaho, with a description of the first oryctodromeus specimens from Idaho. Thesis for Master's Degree. Retrieved January 29, 2013, from Electronic Theses & Dissertations: <http://contentdm.lib.byu.edu/cdm/ref/collection/ETD/id/2317>
- Krumenacker L J, Simon D J, Scofield G, Varricchio D J. 2016. Theropod dinosaurs from the Albian–Cenomanian Wayan Formation of eastern Idaho. *Historical Biol*, 1–17
- Leckie R M, Bralower T J, Cashman R. 2002. Oceanic anoxic events and plankton evolution: Biotic response to tectonic forcing during the mid-Cretaceous. *Paleoceanography*, 17: 13–1–13–29
- Lohmann K C. 1988. Geochemical patterns of meteoric diagenetic systems and their application to studies of paleokarst. In: James N P, Choquette P W, eds. *Paleokarst*. New York: Springer-Verlag. 58–80
- Ludvigson G A, González L A, Fowle D A, Roberts J A, Driese S G, Villarreal M A, Smith J J, Suarez, M B. 2013. Paleoclimatic applications and modern process studies of pedogenic siderite. In: Driese S G, Nordt L C, McCarthy P J, eds. *New Frontiers in Paleopedology and Terrestrial Paleoclimatology*. SEPM Special Publication, 104: 79–87
- Ludvigson G A, González L A, Kirkland J I, Joeckel R M. 2003. A mid-Cretaceous record of carbon isotope excursions in palustrine carbonates of the Cedar Mountain Formation of Utah: Marine-terrestrial correlations of Aptian-Albian oceanic anoxic events 1a, 1b, and 1d. The 3rd International Limnology Congress, Abstract Volume, 169
- Ludvigson G A, Joeckel R M, Gonzalez L A, Gulbranson E L, Rasbury E T, Hunt G J, Kirkland J I, Madsen S. 2010. Correlation of Aptian-Albian carbon isotope excursions in continental strata of the Cretaceous Foreland Basin, eastern Utah, U.S.A.. *J Sedimentary Res*, 80: 955–974
- Ludvigson G A, Ufnar D F, González L A, Carpenter S J, Witzke B J, Brenner R L, Davis J. 2004. Terrestrial paleoclimatology of the mid-Cretaceous greenhouse I: Cross-calibration of pedogenic siderite & calcite $\delta^{18}\text{O}$ proxies at the Hadley cell boundary. *Geol Soc Amer Abstracts Programs*, 36: 305
- Mintz J S, Driese S G, Breecker D O, Ludvigson G A. 2011. Influence of changing hydrology on pedogenic calcite precipitation in vertisols, Dance Bayou, Brazoria County, Texas, U.S.A.: Implications for Estimating Paleoaerospheric PCO_2 . *J Sedimentary Res*, 81: 394–400
- Paton C, Hellstrom J, Paul B, Woodhead J, Hergt J. 2011. Iolite: Freeware for the visualisation and processing of mass spectrometric data. *J Anal At Spectrom*, 26: 2508
- Paton C, Woodhead J D, Hellstrom J C, Hergt J M, Greig A, Maas R. 2010. Improved laser ablation U–Pb zircon geochronology through robust downhole fractionation correction. *Geochem Geophys Geosyst*, 11: Q0AA06
- Petrus J A, Kamber B S. 2012. VizualAge: A novel approach to laser ablation ICP-MS U–Pb geochronology data reduction. *Geostandards Geoanalytical Res*, 36: 247–270
- Schmitt J, Moran M. 1982. Stratigraphy of the Cretaceous Wayan Formation, Caribou Mountains, southeastern Idaho thrust belt. *Rocky Mountain Geol*, 21: 55–71
- Scholle P A, Arthur M A. 1980. Carbon isotope fluctuations in Cretaceous pelagic limestones: Potential stratigraphic and petroleum exploration tool. *AAPG Bull*, 64: 67–87
- Sláma J, Košler J, Condon D J, Crowley J L, Gerdes A, Hanchar J M, Horstwood M S A, Morris G A, Nasdala L, Norberg N, Schaltegger U, Schoene B, Tubrett M N, Whitehouse M J. 2008. Plešovice zircon—A new natural reference material for U–Pb and Hf isotopic microanalysis. *Chem Geol*, 249: 1–35
- Spicer R A, Corfield R M. 1992. A review of terrestrial and marine climates in the Cretaceous with implications for modelling the 'Greenhouse Earth'. *Geol Mag*, 129: 169
- Suarez C A, González L A, Ludvigson G A, Cifelli R L, Tremain E. 2012. Water utilization of the Cretaceous Mussentuchit Member local vertebrate fauna, Cedar Mountain Formation, Utah, USA: Using oxygen isotopic composition of phosphate. *Palaeogeogr Palaeoclimatol Palaeoecol*, 313–314: 78–92
- Suarez C A, Gonzalez L A, Ludvigson G A, Kirkland J I, Cifelli R L, Kohn M J. 2014. Multi-taxa isotopic investigation of Paleohydrology in the lower Cretaceous Cedar Mountain Formation, Eastern Utah, U.S.A.: Deciphering effects of the nevadaplano plateau on regional climate. *J Sedimentary Res*, 84: 975–987
- Suarez M, González L A, Ludvigson G A, Davis J. 2007. Pedogenic sphaerosiderites from the Caballos Formation (Aptian-Albian) of Columbia: A stable isotope proxy for Cretaceous paleoequatorial precipitation. *Geol Soc Amer Abstracts Programs*, 39: 75

- Suarez M B, González L A, Ludvigson G A. 2011. Quantification of a greenhouse hydrologic cycle from equatorial to polar latitudes: The mid-Cretaceous water bearer revisited. *Palaeogeogr Palaeoclimatol Palaeoecol*, 307: 301–312
- Suarez M B, Gonzalez L A, Ludvigson G A, Vega F J, Alvarado-Ortega J. 2009. Isotopic composition of low-latitude paleoprecipitation during the Early Cretaceous. *Geol Soc Am Bull*, 121: 1584–1595
- Tera F, Wasserburg G J. 1972. U-Th-Pb systematics in three Apollo 14 basalts and the problem of initial Pb in lunar rocks. *Earth Planet Sci Lett*, 14: 281–304
- Ufnar D F, A. González L, Ludvigson G A, Brenner R L, Witzke B J. 2002. The mid-Cretaceous water bearer: Isotope mass balance quantification of the Albian hydrologic cycle. *Palaeogeogr Palaeoclimatol Palaeoecol*, 188: 51–71
- Ufnar D F, González L A, Ludvigson G A, Brenner R L, Witzke B J. 2004. Evidence for increased latent heat transport during the Cretaceous (Albian) greenhouse warming. *Geology*, 32: 1049–1052
- Vermeesch P. 2012. On the visualisation of detrital age distributions. *Chem Geol*, 312-313: 190–194
- Vermeesch P. 2004. How many grains are needed for a provenance study? *Earth Planet Sci Lett*, 224: 441–451
- Walker J D, Geissman J W, Bowring S A, Babcock L E. 2013. The geological society of America geologic time scale. *Geol Soc Am Bull*, 125: 259–272
- Whitmeyer S J, Karlstrom K E. 2007. Tectonic model for the Proterozoic growth of North America. *Geosphere*, 3: 220–259
- Wolfe J A, Upchurch Jr. G R. 1987. North American nonmarine climates and vegetation during the Late Cretaceous. *Palaeogeogr Palaeoclimatol Palaeoecol*, 61: 33–77